

metal ions in  
biological systems

**volume 44**

biogeochemistry, availability, and transport of metals in the environment

**edited by**

**Astrid Sigel**  
**Helmut Sigel**  
**and Roland K. O. Sigel**

biogeochemistry, availability, and transport of metals in the environment

biogeochemistry, availability, and transport of metals in the environment

Sigel

**Sigell**

**Sigel**

☐ 1  
☐ 2  
☐ 3  
☐ 4  
☐ 5

ISBN 0-8493-3620-4

cis Group

RES BOOK

ess.com

'States of America

is Assistant Professor (2003) of Inorganic Chemistry at the University of Zürich, with a *Förderungsprofessur* of the Swiss National Science Foundation. His degree *summa cum laude* (1999) from the University of Dortmund, Germany, followed by a postdoctoral fellowship with Professor Rüdiger Lippert, thereafter he spent nearly three years at Columbia University. Newcomer of Anna Marie Pyle (now Yale University); during the six years abroad he worked with various sources. His research focuses on the structural and catalytic properties of ribozymes, especially group II introns and on related topics. He is an editor of the *Inorganic Systems* series since Volume 43.

**verius** Professor (2003) of Inorganic Chemistry at the University of Basel. On various editorial and advisory boards, is involved in European research projects worldwide; he published over 300 articles on metal ion complexes and analogues, coenzymes, and other ligands of biological relevance. He was awarded (2002) by *Inorganica Chimica Acta* (issue 333) among further honours. **Awarded** (Indian Chemical Society, of which he is also an Honorary Fellow, the Chemical Society), a *Doctor of Science honoris causa* degree (Kalyani University, as *Visiting Professor* (e.g., Austria, China, UK) and *Endowed Lectureships*

identified languages and is an editor of the *Metal Ions in Biological Systems* series, together with Hans G. Seiler, Astrid and Helmut Sigel have also edited the *Handbook of Metal Compounds* (1988) and the *Handbook on Metals in Clinical and Analytical Chemistry* (1992). He has also edited together with Ivano Bertini the *Handbook on Metalloproteins* (2001) (all

*availability, and Transport of Metals in the Environment* highlights, supported by charts and tables, the atmospheric transport of metals, the marine biogeochemistry on the carbon cycle, it considers the bioavailability of trace metals in freshwater and soils; it discusses critically the uptake of heavy metals by higher plants, algae and other topics are arsenic in groundwater, the cycling of antimony, the microbial radionuclides, and the biogeochemistry of carbonates which allows insights in the future.

*gical Systems* is devoted to increasing our understanding of the relationship of metals and life processes. The volumes reflect the interdisciplinary nature of metals and life processes. The volumes reflect the interdisciplinary nature of metals and life processes. The volumes reflect the interdisciplinary nature of metals and life processes.

9780849553820

91780849 338205

177. Lloyd JR, Nolting H-F, Solé VA, Bosecker K, Macaskie LE. *Geomicrobiol J* 1998; 15:43-56.
178. Lyalikova NN, Khizhnyak TV. *Microbiology* 1996; 65:468-473.
179. Kashfi K, Lovley K. *Appl Environ Microbiol* 2000; 66:1050-1056.
180. Wildung RE, Gorbey YA, Krupka KM, Hess NJ, Li SW, Pyrmale AE, McKinley JR, Fredrickson JK. *Appl Environ Microbiol* 2000; 66:2451-2460.
181. Lloyd JR, Thomas GH, Finlay JA, Cole JA, Macaskie LE. *Biotechnol Bioeng* 1999; 66:123-130.
182. Peek HD. In: Odom JM, Singleton R., eds. *Sulfate-Reducing Bacteria: Contemporary Perspectives*. New York: Springer-Verlag, 1993.
183. De Luca G, Philip P, Dermoun Z, Rousset M, Vermeiglio A. *Appl Environ Microbiol* 2001; 67:4583-4587.
184. Lovley DR, Coates JD. *Curr Opin Biotechnol* 1997; 8:285-289.
185. Caccavo F Jr, Lonergan DJ, Lovley DR, Davis M, Stolz JF, McInerney JM. *Appl Environ Microbiol* 1994; 60:3752-3759.
186. Gorbey YA, Caccavo F, Bolton H. *Environ Sci Technol* 1998; 32:244-250.
187. Trollope DR, Evans B. *Environ Pollut* 1976; 11:109-116.
188. Friedman BA, Dugan PR. *Dev Ind Microbiol* 1968; 9:381-395.
189. Tsezos M, Remoudaki E, Angelatos V. *Int Biodeterior Biodegrad* 1996; 35:129-154.
190. Bonthrone KM, Basnakova G, Lin F, Macaskie LE. *Nature Biotechnol* 1996; 14:635-638.
191. Taghavi S, Mergeay M, Nies D, Van der Leije D. *Res Microbiol* 1997; 148:536-551.
192. Amachi S, Kasahara M, Hanada S, Kainagata Y, Shinoyama H, Fujii T, Muramatsu Y. *Environ Sci Technol* 2003; 37:3885-3890.
193. Councell TB, Landa ER, Lovley DR. *Water Air Soil Pollut* 1997; 100:99-106.
194. Fuse H, Inoue H, Murakami K, Takimura O, Yamaoka Y. *FEMS Microbiol Lett* 2003; 229:189-194.
195. Truesdale VW, Watts SF, Rendell AR. *Deep-Sea Res Part I-Oceanogr Res Papers* 2001; 48:2397-2412.
196. Muramatsu Y, Yoshida S. *Geomicrobiol J* 1999; 16:85-93.

## 9

## Biogeochemistry of Carbonates: Recorders of Past Oceans and Climate

Rosaling E. M. Rickaby<sup>1</sup> and Daniel P. Schrag<sup>2</sup>

<sup>1</sup>Department of Earth Sciences, University of Oxford,  
Parks Road, Oxford, OX1 3PR, UK

<sup>2</sup>Laboratory for Geochemical Oceanography,  
Department of Earth and Planetary Sciences, Harvard University,  
20 Oxford Street, Cambridge, Massachusetts 02138, USA

1. Introduction to Biogenic Carbonate Proxies	242
2. Partition Coefficients	244
3. Recorders of Past Ocean Conditions	246
4. Biomineralization Processes of Different Organisms	249
4.1. Coccolithophores	249
4.2. Perforate Foraminifera	251
4.3. Corals	252
4.4. Biomineralization and Proxies	252
5. Biological Discrimination Between Calcium and Trace Metals	254
5.1. Selectivity of Ion Channels	254
5.2. Selectivity of Ion Pumps	256
5.3. Selectivity of Acidic Polysaccharide Template	260
5.4. Biomineralization Selectivity: A Hypothesis	261
6. Biological Ion Selectivity and the Environment	262
6.1. Temperature	263
6.2. Kinetics	264

7. Summary	265
Acknowledgments	266
Abbreviations	266
References	266

## 1. INTRODUCTION TO BIOGENIC CARBONATE PROXIES

This chapter will address the use of trace metals in biogenic carbonates as proxies for past ocean conditions with an emphasis on the biogeochemistry of biomineralization. Our aim is to illustrate the utility of trace metal proxies for reconstructing ocean conditions in the past, but also to emphasize how little is known about the detailed mechanisms that underlie these proxies.

In order to probe the record and forcing mechanisms of past climate change beyond the range of direct observation and historical accounts, we are forced to rely on chemical or isotopic proxy records for different ocean properties such as temperature, nutrient abundance, or primary productivity. These proxy records are often in the form of chemical variations encapsulated within exquisitely crafted biomineralized carbonates. The biogenic calcium carbonate minerals, calcite, and aragonite, have an incredibly flexible chemistry. Variations in the abundance of the heavy isotope relative to the light isotope of both O and C ( $\delta^{18}\text{O}$ , and  $\delta^{13}\text{C}$ ) in the  $\text{CO}_3^{2-}$  ion can be frozen within these minerals (e.g., [1–3]). Divalent cations of a similar ionic radius (Mg, Sr, Ba, Mn, Fe, Cu, Zn, Cd) can substitute for  $\text{Ca}^{2+}$  in the crystal structure (e.g., [4]) and significant levels of U, Li, B, and Na have also been found in carbonates. With the recent advent of multi-collector inductively coupled mass-spectrometry (MC-ICPMS) in the last 10 years, it has become possible to resolve sub per mill (part per thousand) fractionations in the stable isotopes of elements heavier than C and O such as Fe (e.g., [5,6]) or Mo (e.g., [7,8]). A new avenue of research is developing methodologies for the development and application of Ca isotopic variations ( $\delta^{44}\text{Ca}$ ) and even isotopic variations in the metals that can substitute for  $\text{Ca}^{2+}$  (e.g.,  $\delta^{26}\text{Mg}$ ,  $\delta^{68}\text{Zn}$ , and  $\delta^{57}\text{Fe}$ ) as proxies for the past (e.g., [9]).

The information we derive from chemical proxies depends on the residence time of the chemical in the ocean relative to the timescale of interest and the  $\sim 1.5$  kyo year (kyr) mixing time of the ocean. Elements with a relatively short residence time in the ocean have a non-uniform distribution in seawater, which can be indicative of nutrient-like behavior, conservative mixing, or scavenging onto particles. If these elements are then incorporated into biogenic carbonates in direct proportion to their concentration in seawater, they can provide a proxy for reconstructing those processes in the past. For example, the Cd concentration of seawater correlates with phosphate (an essential nutrient) in the ocean with near total depletion in surface waters and enrichment at depth. As a result

Cd/Ca ratios have been used to reconstruct phosphate concentrations in the past both in planktonic foraminifera to measure productivity in surface waters (e.g., [10]), and in benthic foraminifera to monitor changes in the characteristic nutrient signatures of deep water masses and the pattern of ocean circulation (e.g., [11]). For elements where the residence time in the ocean is long relative to the timescale of interest, any variation in the concentration or isotopic value recorded by a biogenic carbonate must be related to factors controlling the partitioning or isotopic fractionation into the carbonate shell such as temperature, salinity, or growth rate. As an example, Mg has a residence time of  $\sim 5$  million year (Myr), but Mg/Ca varies significantly between glacial and interglacial periods (100 kyr) and is used as a paleothermometer and paleosalinity proxy (in concert with  $\delta^{18}\text{O}$ ) on these timescales (e.g., [12–14]). One final application is when the timescale of interest is long relative to the residence time of the element and it is incorporated into the carbonate in direct proportion to its concentration or signature in seawater. In this case, the chemical proxy can reveal changes in the oceanic budget of that element. For example, the Sr isotope curve ( $^{87}\text{Sr}/^{86}\text{Sr}$ ) measured in marine carbonates on long timescales (e.g., 75 Myr) tells us about the changes in continental weathering processes [15].

With the exception of some systems such as strontium isotopes, the isotopic or chemical fractionation between seawater and the biogenic carbonate almost always involves biological control which is poorly understood. This means that there exists a persistent doubt as to the reliability of these proxies as some have argued that only a full mechanistic understanding of the incorporation of trace metals into biogenic carbonates would allow truly accurate reconstruction of past environments. At the same time, careful calibrations with laboratory or field observations have led to the production of a wide range of proxy records which have provided useful information about past climates and ocean conditions. This highlights the challenge that confronts the paleoceanographer who must work to develop the deepest level of mechanistic understanding of how chemical and isotopic signals are incorporated in biogenic carbonates, but at the same time must continue to use those proxies with the best knowledge available to test hypotheses about ancient climates.

In this chapter, we discuss the comparative trace metal geochemistries of coccolithophores, foraminifera, and corals relative to inorganic calcite and aragonite respectively, in order to define the differing nature of biological selectivity. We then address the biomineralization process for each organism and the biochemical nature of the trace metal selectivity involved at each step of the biomineralization. This overview allows us to develop a mechanistic framework within which to consider trace metal proxies in biogenic carbonate. Notably, the biochemical selectivity is based on similar chemical constraints to those of an inorganic crystal. In each case, the geometry of coordinating oxygens defines a cation specific site with a Ca–O bond length of between 2.2–2.6 Å, but the biochemical process adds a further selectivity due to the energy of dehydration of a

cation before binding to the site. We propose that the vital effects of trace metal uptake are related to the varied energy required to dehydrate cations.

## 2. PARTITION COEFFICIENTS

The origins of chemical proxies for paleoceanography originates from the treatment of carbonate minerals as inorganic materials. The application of thermodynamics to geology in the 1960s created the vision that with a complete understanding of the thermodynamic partitioning of metals into carbonate minerals, the environmental variables (temperature, saturation state) could be calculated from measurements of sediments for various times in the past [16–18].

The true inorganic partition coefficient for trace metal uptake into carbonate, or the isotopic fractionation factor for stable isotopes, is related to the equilibrium partitioning of the particular element or isotope between seawater and calcium carbonate. A partition coefficient greater (less) than one implies that the carbonate is enriched (depleted) in that metal or isotope relative to the seawater content. In inorganic systems, the theoretical partition coefficient is generally agreed to relate to the quotient of the solubility product of  $\text{CaCO}_3$  and  $\text{MCO}_3$  [19–21] and to the activity of the cations in water. In reality, experimental conditions during inorganic precipitation of minerals only approximate equilibrium.

Experimental partition coefficients are affected by kinetic processes relating to the adsorption of the trace metal to kink sites on the growth steps of an actively growing crystal, and also solution boundary related processes. For the incorporation of divalent cations into inorganic calcite, there is a correlation between the experimental partition coefficient and the effective ionic radius in sixfold coordination (Fig. 1). The experimental partitioning of the cations  $\text{Mg}^{2+}$ ,  $\text{Co}^{2+}$ ,  $\text{Fe}^{2+}$ ,  $\text{Mn}^{2+}$ ,  $\text{Cu}^{2+}$ ,  $\text{Zn}^{2+}$ , and  $\text{Cd}^{2+}$ , which have ionic radii less than that of  $\text{Ca}^{2+}$  and form rhombohedral carbonates, increases with increasing effective ionic radius towards that of  $\text{Ca}^{2+}$ .  $\text{Cd}^{2+}$  (the element with the most similar ionic radius to Ca) provides a maximum to the partition coefficient, and the trend then decreases with increasing effective ionic radius away from  $\text{Ca}^{2+}$  to the cations  $\text{Sr}^{2+}$ , and  $\text{Ba}^{2+}$  which have ionic radii larger than  $\text{Ca}^{2+}$ , do not fit the lattice so easily and tend to form orthorhombic carbonates. In general, ions with a similar but smaller radius than  $\text{Ca}^{2+}$  have the highest partition coefficient and the ions which fit least well into the  $\text{Ca}^{2+}$  sites have lower partition coefficients.

The original application of equilibrium thermodynamics to biogenic carbonates was done with the awareness of the possible complications from the biomineralization process [1]. These complications were treated by assuming that thermodynamic equilibrium was the underlying physical process, and that any offset from equilibrium was incorporated into a correction that was called the "vital effect" (and was usually assumed to be constant). There was good reason to make this assumption as some experimental data supported this

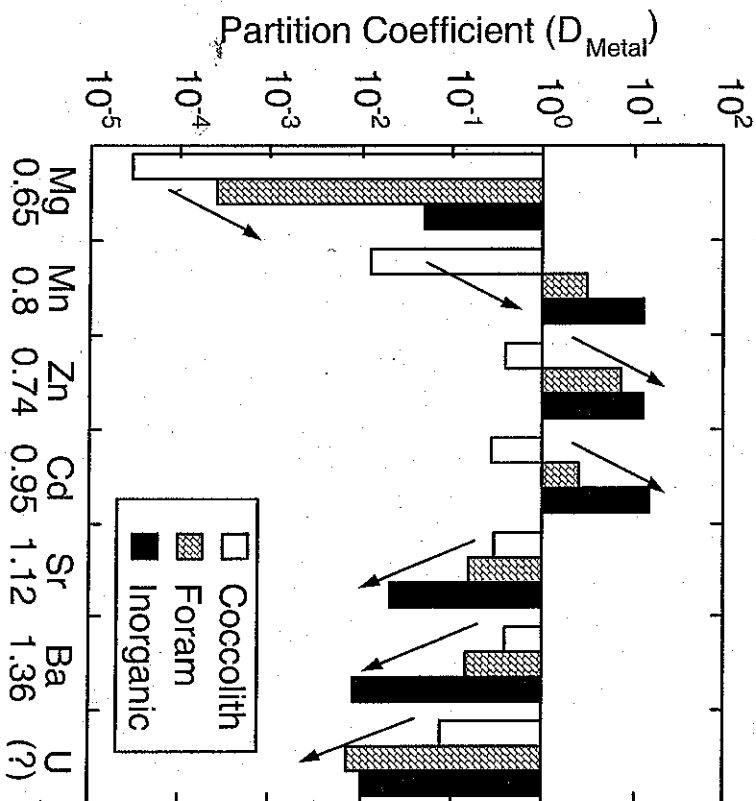


**Figure 1** Partition coefficients for a range of metals for inorganic (black bars), foraminifera (brick bars) and coccolith (open bars) calcite. The inorganic calcite and foraminifera partition coefficients are taken from Reis [22,23]. There is some variance but the graph is not changed significantly as it is plotted on a log scale. The partition coefficients for coccolithophores are based on trace metal analyses of cultured coccolithophores [Rickaby R. E. M., unpublished results]. The ionic radius of each metal in Å is also indicated except for uranium. For most of the metals, we can assume that the metal substitutes for  $\text{Ca}^{2+}$  in its divalent state. At present there is uncertainty as to the form by which U substitutes into the calcite lattice. There is speculation that it occurs in the form  $\text{UO}_2^{2+}$  [24] but this is as yet unproven.

view, such as the variation of oxygen isotopes with temperature in foraminifera that showed constant offsets between species (e.g., [3]). In much current work in paleoceanography, equilibrium thermodynamics in inorganic minerals is still presumed to be the underlying mechanism responsible for the preservation of environmental information (e.g., [25]).

That the pattern of trace metal uptake in biogenic carbonate resembles the inorganic system suggests that either inorganic calcite partitioning is still the dominant control on trace metal uptake into biominerals or that similar kinetic

and thermodynamic chemical laws which govern crystal selectivity between  $\text{Ca}^{2+}$  and a similar trace metal also govern biological selectivity. However, there are differences in selectivity associated with the vitality of these processes which probably arise due to the greater number of steps involved in the biological precipitation process (Fig. 1). For cations which are smaller than  $\text{Ca}^{2+}$ , the effect of the biology is to discriminate more effectively than inorganic calcite, which implies a greater selectivity during ion transport to the site of nucleation and precipitation. For cations which are larger than  $\text{Ca}^{2+}$ , the biological discrimination is not as efficient and the biological partition coefficients tend to be greater than the inorganic coefficients. An alternative explanation than reliance on ionic radius alone for these effects is that the smaller ions are "biologically important" metals and often form the metallic co-factors for essential enzymes. Therefore, it could be argued that biological processes are able to recognize and better select amongst the biologically relevant cations.

Further evidence for a non-inorganic imprint on the chemistry of biogenic carbonate is the sensitivity of trace metal uptake to a wider array of environmental factors than one would predict from thermodynamics alone. Not only are the partition coefficients for biological carbonates different than inorganic carbonates by orders of magnitude, but the sensitivity to the environment, e.g., temperature, can be greater or smaller by orders of magnitude or even have an opposite sense (Fig. 2). Most importantly, the investigation of biomineralization over the last two decades [26] has shown a remarkable degree of active transport and control over every step in the biomineralization process. This suggests that whatever fractionations may exist, either in trace metals or isotopes, they are affected by preferential transport, and that the thermodynamic partitioning into inorganic calcite is not the most appropriate context within which to consider trace metal proxies.

### 3. RECORDERS OF PAST OCEAN CONDITIONS

A comprehensive overview of recent proxies has been provided by Henderson [27]. We will not provide a review here, except to mention briefly some of the applications of the groups of organisms discussed later. However, it is valuable to remember that the motivation in developing new chemical or isotopic proxies is to reconstruct environmental variables in ancient oceans. Therefore, the efforts at exploring the biophysical mechanisms that underlie these proxies have often been pushed aside in favor of simple calibration experiments in which correlations are embraced without a deep understanding of causation. Such efforts have provided a wealth of information about the history of the oceans and climate, but their reliability must ultimately be assessed in the context of a deeper understanding of mechanisms.

Our ultimate goal in reconstructing past climate change is to enhance our understanding of the climate system to create better predictions for the future. From this perspective, we must record changes on timescales which range

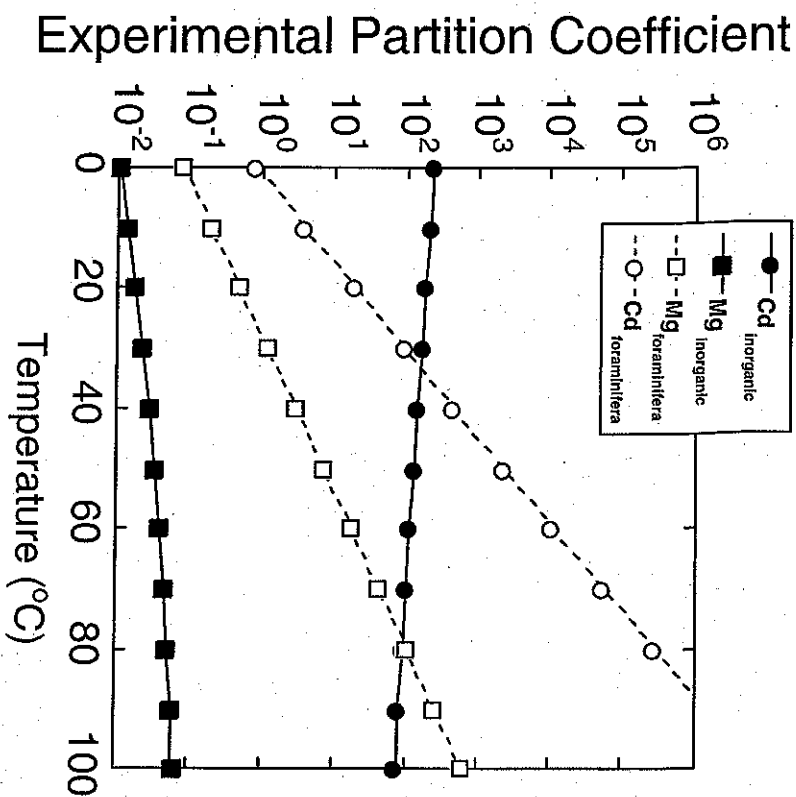


Figure 2 Theoretical and empirical variations of partition coefficients for  $\text{Mg}^{2+}$  (squares) and  $\text{Cd}^{2+}$  (circles) into inorganic calcite (open symbols) based on the calculations reported in Ref. [22], and for planktonic foraminifera (closed symbols) [10,12].

across eight orders of magnitude. Later we select just a few examples to illustrate the sort of information we are gaining from biomimetal trace metal proxies.

In order to monitor the reaction of our climate system to the exponentially increasing input of greenhouse gases since the industrial revolution, we require information from the subannual, decadal, and century scale. Coral skeletons can grow at rates of up to 10 cm/yr which allow for high resolution annual records, continuous for hundreds of years in some circumstances. Trace metal proxies from coralline aragonite based on  $\text{Mg}/\text{Ca}$ ,  $\text{Cu}/\text{Ca}$ ,  $\text{Mn}/\text{Ca}$ , and  $\text{Cd}/\text{Ca}$  all yield seasonal information about upwelling and El Niño (e.g., [28–30]), but above all  $\text{Sr}/\text{Ca}$  in coral aragonite is the most extensively used paleothermometer. For example a unique insight of interdecadal variability associated with the industrial revolution within the Pacific has been afforded by records

of coral Sr/Ca from across the Pacific which span the last 300 years [31]. These temperature records in the Pacific suggest that the spatial pattern of the inter-decadal Pacific oscillation at least in the South Pacific has varied considerably and undergone a major reorganization at ~1880 AD.

To investigate oceanic conditions associated with abrupt suborbital events, and Milankovitch forced glacial-interglacial cycles which yield insight as to how the climate alters under naturally forcing, we require information on the time-scale of thousands to hundreds of thousands of years. The rain of foraminifera and coccolithophores, amongst other components to ocean sediments accumulate at an average rate of 1–4 cm/kyr, but can be as high as 50–100 cm/kyr so down-core analysis of their chemistry is well suited for reconstructing ocean conditions on these timescales and can be extended into the millions of years by drilling of sediments. Amongst a host of other trace metal proxies in foraminifera, the Mg/Ca paleothermometer and paleonutrient proxy Cd/Ca are perhaps the most prevalent. As an example, Mg/Ca can be used in concert with  $\delta^{18}\text{O}$  to resolve temperature and salinity variations in planktonic forams for surface conditions, and benthic forams for deep water signatures. This combined proxy has been used to focus on the role of thermohaline overturning during millennial scale cooling events which punctuate the last glacial cycle and the most recent transition from glacial to interglacial conditions, ~10 kyr ago. In particular, salinity within the surface of the Caribbean Sea, the main source of surface waters feeding North Atlantic deep water (NADW) formation have been shown to vary in concert with the strength of NADW flow [14]. Furthermore, benthic records across the rapid climate changes of the glacial-interglacial transition from 3146 m in the North Atlantic reveal an oscillation between the changing local dominance of warm, high salinity NADW vs. cold, low-salinity southern-sourced Antarctic bottom water (AABW) associated with stadial and interstadial variations in the Greenland ice core [32]. This reinforces existing thinking that variations in the strength of NADW are intricately linked to millennial scale climate variations as evidenced by benthic foraminiferal Cd/Ca tracing the distinctive nutrient signatures of nutrient poor NADW and nutrient rich AABW (e.g., [33]). Returning to surface waters, planktonic foraminiferal Cd/Ca records from the Southern Ocean refute that increased iron fertilization of productivity in these nutrient rich waters at glacial times could have been responsible for the glacial draw-down of carbon dioxide [10].

The trace metal content of coccolithophores yields information on the same timescales to foraminifera, but about different aspects of the ocean due to the contrasting geochemistry of their biomineralization. The full range of trace metals from coccolithophore calcite in the sediments have not been exploited due to difficulty in separating them from potentially contaminating clays. Nonetheless, Sr/Ca is unaffected by such contamination and correlates with the growth rate of coccolithophores [34–36] and can therefore divulge past productivity of the oceans (e.g., [37]). We can therefore use proxy records from foraminifera and coccolithophores to investigate the past when atmospheric carbon

dioxide was analogous to our current situation, as the globe oscillated between an icehouse and ice free greenhouse world on timescales of tens of millions of years. A novel methodology has been developed to probe the climate and ocean hundreds of millions of years ago before foraminifera and coccolithophores had evolved. Trace metal ratios (Mg/Ca, Sr/Ca, and Na/Ca) in parallel with stable isotopes from belemnites (cephalopod molluscs which were abundant in the Jurassic ocean) are starting to provide temperature and salinity information (e.g., [38]). These organisms are now extinct and so we have no real calibration data, or information regarding biomineralization mechanisms and as such will not be discussed further.

This is by no means a comprehensive review of how trace metal proxies within biominerals have enhanced our understanding of the past climate, but an illustration of how we can probe a range of climatically important timescales and use different trace metals to explore an assortment of characteristics of the past ocean.

#### 4. BIOMINERALIZATION PROCESSES OF DIFFERENT ORGANISMS

We now seek to address whether the contrast in trace metal geochemistry of biogenic carbonates vs. inorganic carbonates can be understood in terms of the different processes which are important to the biomineralization mechanism of different organisms. First, we shall summarize the biomineralization process of coccolithophores, foraminifera and corals [Fig. 3(a–c)]. The fossil remains of each of these organisms make a significant contribution to our paleoceanographic reconstructions of the past world.

##### 4.1. Coccolithophores

Coccolithophores are single-celled plant plankton which belong to the phylum Haptophyta, and secrete an interlocking sphere of calcite platelets [Fig. 3(a)]. A physical mechanism for the assembly and extrusion of a coccolith has been proposed by Westbroek et al. [39], detailed in Refs. [40,41], and summarized by Young and Henriksen [42].

Growth occurs in a coccolith vesicle derived from the Golgi body and which is supplied with matrix material and calcium via Golgi vesicles. The biomineralization process commences with formation of an organic scale within a vesicle which develops into a complex form, with extensions containing dense particles termed coccolithosomes. The coccolithosomes appear to play a key role in calcification and have been shown to be complexes of acidic polysaccharides with calcium ions [43]. It is thought that they function as calcium vectors during biomineralization and that the polysaccharide phase forms the crystal coatings. Nucleation of a protococcolith ring of alternating orientation simple crystals then occurs around the rim of a precursor base-plate scale followed by crystal growth upward and outward to form the complex crystal



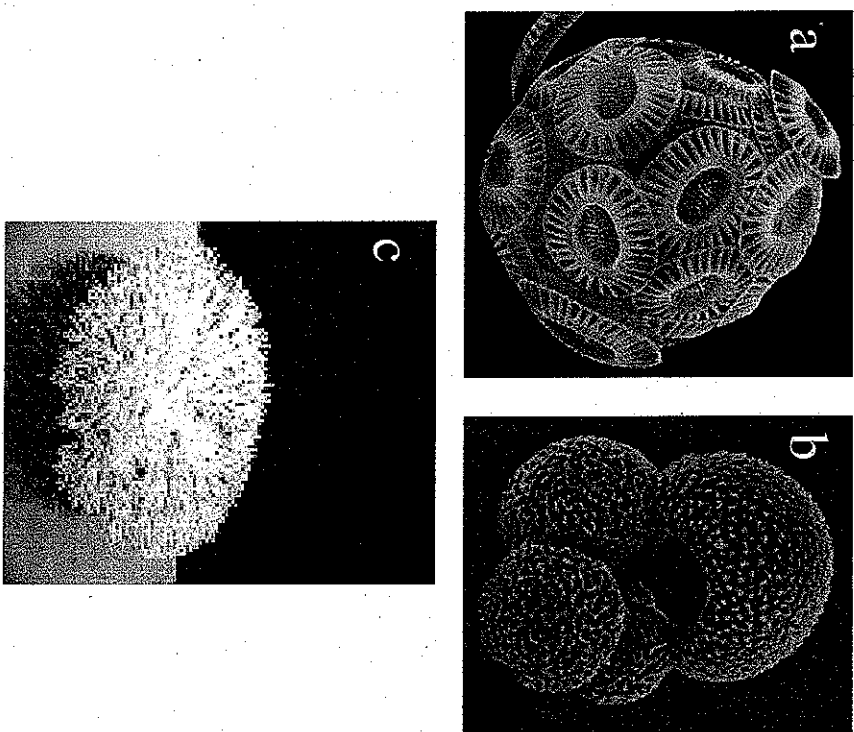


**Figure 3** Scanning electron microscopy (SEM) photos of (a) *Emiliana huxleyi* measuring  $\sim 10$   $\mu\text{m}$  in diameter, (b) *Globigerina bulloides* measuring  $\sim 250$   $\mu\text{m}$  in diameter, (c) a coral measuring  $\sim 10$  cm in diameter.

units of the complete coccolith. Assembly of the coccolith, which consists of a cycle of radially and vertically oriented calcite crystals, involves a folded acidic polysaccharide matrix [44]. This polysaccharide matrix is thought to promote and mold calcification by providing uranic acid groups as nucleation sites for  $\text{Ca}^{2+}$ , but also inhibits crystal growth by adhering to the surface of the coccolith when construction is complete [39]. This organic matrix framework can provide binding sites for the components of a mineral, selectively nucleating specific crystallographic faces, and organic carrier molecules can ensure supersaturation of a phase within mineralizing compartments.

The coccolith grows in an expanding vesicle and much of the morphology is a product of interaction between adjacent crystals. The final structure of the

completed coccolith is an emergent result of inorganic growth of crystals defined by the nucleation stage, within a space defined by an expanding organic vesicle. After completion of the coccolith, the vesicle dilates and at this stage, a dense organic coating is visible around and between the coccolith crystals. It is reasonable to infer that the final coating of polysaccharides that can prevent dissolution of the element also serves to inhibit crystal growth. The coccolith is then exocytosed onto the surface to form an interlocking sphere of coccoliths by fusion of the vesicle membrane and cell membrane.

#### 4.2. Perforate Foraminifera

Foraminifera are unicellular calcifying marine amoeba, taxonomically part of the Protista. The most common arrangement is spherical coiling [Fig. 3(b)] with planispiral or low trochispiral tests. Erez [45] summarizes the major steps involved in perforate foraminifera calcification.

In perforate foraminifera, the first step for chamber formation involves delineation of a space using ectoplasmic pseudopods. The next step is to define the shape of the newly formed chamber by creating a cytoplasmic bulge that serves as a mold for the organic matrix and as a template for nucleation. The third step is the precipitation of  $\text{CaCO}_3$  on both sides of a thin organic layer. Radiotracer experiments [46] have confirmed the presence of an internal Ca pool which foraminifera use for this calcification. It is possible that this Ca pool may be connected to small polarizing granules that were recently observed in the endoplasm [47]. Ca is concentrated in the endoplasm in a highly soluble, birefringent mineral phase composed of Ca, Mg, P, and S. The granules are membrane bound and may contain organic matrix or some of its components. The granules provide Ca for the first  $\text{CaCO}_3$  crystals that precipitate over the newly formed organic matrix. At this stage the chamber consists of a two-dimensional primary wall made of Mg-rich spherulites embedded within the organic matrix.

The second stage of calcification involves massive deposition of a low Mg-calcite wall. This secondary calcite is made of layered crystal aggregates with their *c*-axis perpendicular to the test wall. These units form the secondary lamination and are responsible for the bulk of the skeleton deposition because foraminifera cover their preexisting shell with a new layer of calcite every time a new chamber is built. The biomineralization process forming secondary calcite involves vacuolization of seawater and its modification within the cytoplasm perhaps to reduce the Mg/Ca ratio and elevate the pH. In order to precipitate low Mg-calcite, it is necessary to either concentrate Ca or reduce Mg in the seawater vacuole (as well as increase the pH). The main possibilities considered involve active pumping away of Mg, or alternatively complexation by organic materials perhaps the pseudopodial network (bilipid membranes). Towards the end of their life cycles, many planktonic foraminifera deposit several different types of  $\text{CaCO}_3$  often in the form of a thick crust as is termed gametogenic calcite.

#### 4.3. Corals

Reef corals [Fig. 3(c)] belong to the order Scleractinia, all of which accrete hard exoskeletons. The animal responsible for skeletal formation is the polyp, a double-walled sack of simple design [48].

The calicoblastic layer of the ectoderm, which lies adjacent to the skeletal surface, is considered to be involved in some way in calcification. The basic building blocks of the coral skeleton consist of fine aragonite crystals arranged in three-dimensional fans about a calcification center. Within the calcification centers are submicron sized granular crystals bundled into discrete "nuclear packets". The small size of these granular seed crystal may indicate intracellular mineralization, as suggested by Hayes and Goreau [49]. It is probable that the contents of intracellular vesicles are transported across the apical membrane and exocytosed into the calcifying space. Indeed, this is a likely route for seawater entry. One further suggestion is that the intracellular vesicles in the apical membrane of the calicoblastic ectoderm, with their organic contents, are sites of production and stabilization of amorphous  $\text{CaCO}_3$  precursors of the granular seed crystals that occupy the centers of calcification. The geometry of the nuclear packets indicates that they are incorporated into the skeleton in a non-rigid state [50].

Calcium ions enter the coral's calcifying space by both passive and active transport [51,52]. Passive entry occurs by way of seawater transported via invaginated vacuoles leaking or diffusing into the calcifying space. Active transcellular transport of both ions occurs enzymatically, via the  $\text{Ca}^{2+}$  ATPase pump. Regarding the control on precipitation, the origin, physical structure, and function of the putative organic matrix in coral skeletons remains elusive. A model proposed by Barnes [53] argues that fast growing crystals precipitated from a supersaturated solution will compete with each other. The tendency for these crystals to diverge from the optimum axis of growth gives rise to three-dimensional fans. Further compelling evidence for the predominance of physico-chemical factors in the growth of aragonite fibers is the correlation between fiber morphology and coral growth rate [54].

The range of fiber morphologies found amongst the scleractinian taxa could be explained by basic theories of crystal growth in inorganic systems without the need for mediation by an organic macromolecular framework or matrix. Recently however, Cuif et al. [55] have proposed a polycyclic model of crystal growth, involving step-by-step growth of aragonite fibers, each step initiated and guided by a sulfated organic matrix sheet. Alternatively sheets of sulfated organic materials at daily growth boundaries could be inhibitory rather than promotional features.

#### 4.4. Biomineralization and Proxies

It is interesting to note the gradation between the chemistry of inorganic calcite, planktonic foraminifera and the biologically extreme chemistry of coccolith

calcite from Fig. 1, i.e., the coccolith calcite experiences the greatest biological influence. Furthermore, all coccolith calcite partition coefficients are less than 1. This corroborates the extreme biological influence on the coccolith calcite and argues for greater selectivity between calcium and trace metals. By contrast, a coral skeleton largely resembles the chemistry that would be expected from inorganic precipitation from seawater. Most trace elements and even small particles occur in the skeleton in proportions reflecting their abundance in seawater, and their tendencies to become incorporated either within or among aragonite crystals. The trace metal geochemistry of corals reflects minimal biological influence. It appears that biomineralization controls the chemistry of biogenic carbonates to differing degrees for different organisms. These differences are easily explained by the relative involvement of biological transport and matrix-mediated precipitation, i.e., coccolithophores experience the most involved intracellular precipitation compared to forams and corals (Fig. 4). There is an importance of seawater vacuolization for both corals and foraminifera, but this process is not thought to occur in coccolithophores. By contrast, organic matrix-mediated precipitation in coccolithophores is key but its

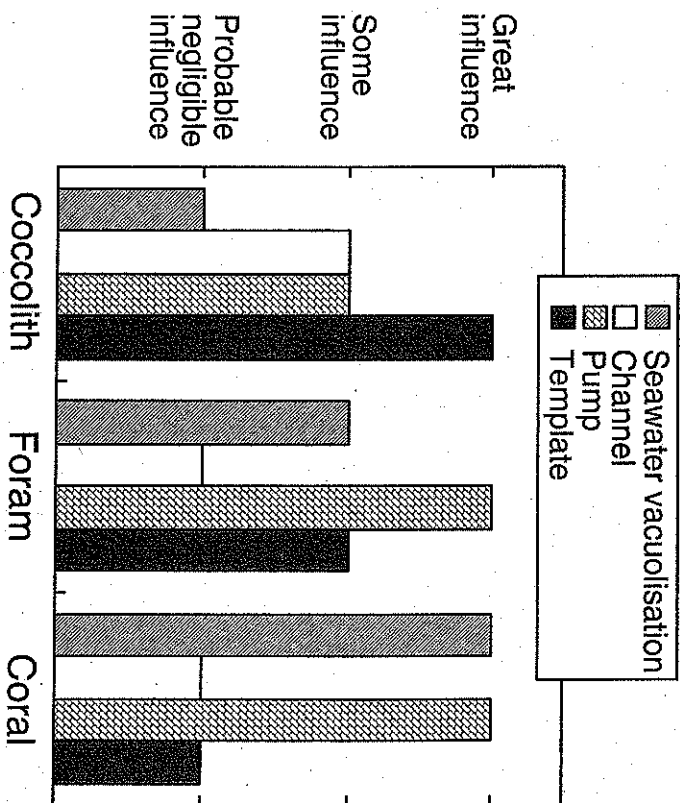


Figure 4 A figure to summarize the relative influences of  $\text{Ca}^{2+}$  channels (open bars),  $\text{Ca}^{2+}$  pumps (brick bars), the template (filled bars), and seawater vacuolization (diagonally hatched bars) on the biomineralization process in coccoliths, corals, and foraminifera.



importance is less for foraminifera and is still questioned in corals. The relative trace metal chemistries of coccolithophores, foraminifera, and corals undoubtedly reflect the differing degrees of biological control on the precipitation.

## 5. BIOLOGICAL DISCRIMINATION BETWEEN CALCIUM AND TRACE METALS

In our quest to understand the mechanisms that account for the different geochemistries of biominerals, we now turn our attention to the trace metal discrimination characteristics of the transport and assemblage processes. Calcium plays a dual role in biomineralizing organisms as both a substrate for calcification and an intracellular regulator.

The cytosol concentration of free calcium is rigorously controlled and maintained at a very low level. For our biological end-member calcite, i.e., the coccolithophores, the  $\text{Ca}^{2+}$  ions necessary for the formation of calcite diffuse from seawater through  $\text{Ca}^{2+}$ -selective channels into the cytosol of the coccolithophore driven by a potential difference and by a very low  $\text{Ca}^{2+}$  activity in the cytosol (0.1  $\mu\text{M}$ ) (Fig. 5). This low cytosolic concentration of  $\text{Ca}^{2+}$  means that  $\text{Ca}^{2+}$  must be pumped against a concentration gradient at some stage during its transport to the site of precipitation in order to attain saturation. Although this process must be extremely selective for  $\text{Ca}^{2+}$  ion, the very presence of trace metals in coccolith calcite indicates that the similarly sized trace metal ions must substitute for  $\text{Ca}^{2+}$  and be transported via the same mechanism but at a different rate as  $\text{Ca}^{2+}$ .

More generally, the two steps which must impact biogenic calcite chemistry are the transport of ions from seawater across membrane(s) to the site of precipitation, and, the precipitation of the calcite on an organic matrix (Fig. 5). One or both of these processes is common to all biomineralizing organisms. Transport of ions across a membrane is driven by pumps against a concentration gradient or directed through channels when transport is with a concentration gradient. Channels and pumps have very different modes of selectivity and transport. Similarly, the intricate relationship between the molding and precipitation control of the organic template or matrix may control the selection of ions during assemblage of the mineral.

### 5.1. Selectivity of Ion Channels

Highly specific membrane spanning macromolecular structures, ion channels, serve to facilitate and control the passage of selected charged ions across the hydrocarbon lipid barrier down a concentration gradient. Three divalent ions,  $\text{Ca}^{2+}$ ,  $\text{Sr}^{2+}$ , and  $\text{Ba}^{2+}$ , pass readily through all known  $\text{Ca}^{2+}$  channels. Most other divalent ions act as blockers of  $\text{Ca}^{2+}$  channels, but in isolated cases, inward currents carried by  $\text{Mg}^{2+}$ ,  $\text{Mn}^{2+}$ ,  $\text{Co}^{2+}$ ,  $\text{Zn}^{2+}$ , or  $\text{Ba}^{2+}$  have been demonstrated [56–58]. The selectivity of an ion-selective channel for divalent ions

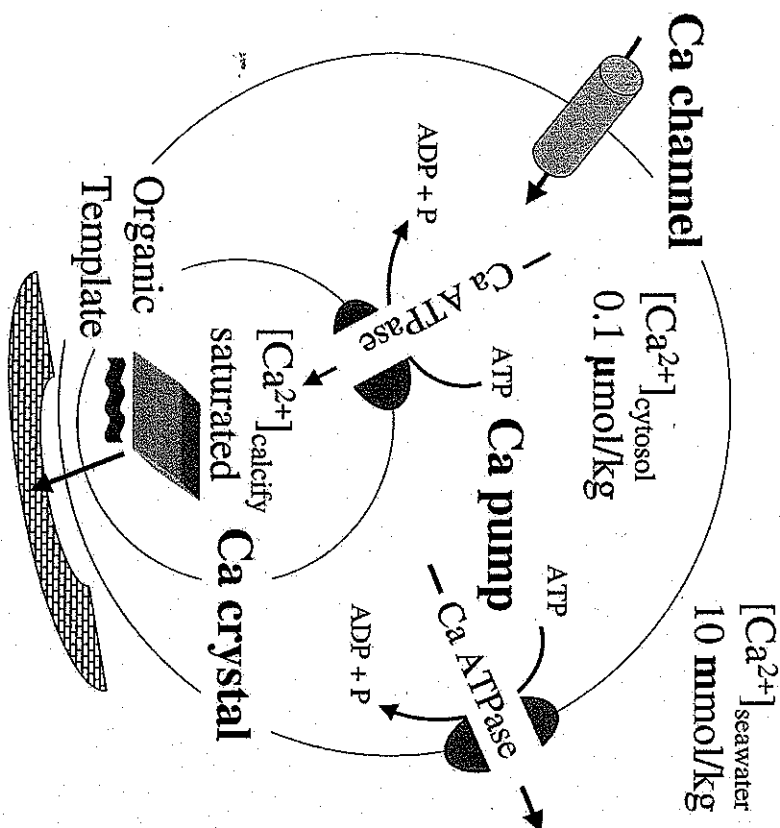


**Figure 5** Schematic representation for the most biologically involved precipitation of calcite to show the involvement of  $\text{Ca}^{2+}$  channels (from high to low  $\text{Ca}^{2+}$  concentration),  $\text{Ca}^{2+}$  pumps (from low to high  $\text{Ca}^{2+}$  concentrations) and the involvement of the template as well as the final stage of crystal precipitation. All calcite biomineralization processes will involve at least one or more of these steps.

follows the sequence  $\text{Ca}^{2+} > \text{Sr}^{2+} > \text{Ba}^{2+} \gg \text{Mg}^{2+}$  ( $\text{Ca}^{2+} > \text{Sr}^{2+} \sim \text{Ba}^{2+} \gg \text{Li}^+ > \text{Na}^+ > \text{K}^+ > \text{Cs}^+$ ) (see Table 1). However, the selectivity of channels is governed by two factors, partitioning into the membrane and mobility once inside. As a result, for some channels the current of  $\text{Ba}^{2+}$  through the channel can be greater than that of the more selected  $\text{Ca}^{2+}$  or  $\text{Sr}^{2+}$ .

Although no detailed molecular structure has been published for a  $\text{Ca}^{2+}$  channel, many analogies regarding selectivity may be drawn from the study of a  $\text{K}^+$  channel by Doyle et al. [59]. If a channel is highly ion-selective, the pore must be narrow enough to force permeating ions into contact with the wall so they can be sensed. These narrow ion selective regions of ion channels are known as the selective filter. Doyle et al. [59] showed that a  $\text{K}^+$  channel

**Table 1** Permeability Ratios  $P_x/P_{Ca}$  for L-Type Ca Channels<sup>a</sup>

Ion	$P_x/P_{Ca}$	Ion	$P_x/P_{Ca}$
Ca	1.0	Li	1/424
Sr	0.67	Na	1/1170
Ba	0.40	K	1/3000
		Cs	1/4200

<sup>a</sup>An L-type Ca channel has a large single-channel conductance and a long-lasting current.

begins as a tunnel and then opens into a wide cavity near the middle of the membrane. A  $K^+$  ion would move throughout the internal pore and cavity and still remain mostly hydrated. The chemical composition of the wall lining the pore is predominantly hydrophobic. In contrast, the narrow selectivity filter is lined exclusively by polar main chain atoms belonging to amino acids. So, the selectivity is maintained due to two critical structural factors. When an ion enters, it dehydrates nearly completely. To compensate for the energetic cost of dehydration, the carbonyl oxygen atoms must take the place of the water oxygen atoms, come in very close proximity and coordinate as strongly as the water (Fig. 6).

Secondly, the interactions and hydrogen bonds between surrounding proteins seem to act like a layer of springs stretched radially outwards to hold the pore open at its proper diameter. Smaller or larger ions would distort this structure and disrupt the energy balance. Finally, two  $K^+$  ions at close proximity in the selectivity filter repel each other. The repulsion overcomes the otherwise strong interaction between ion and protein and allows rapid conduction in the setting of high selectivity. This feature is common to  $Ca^{2+}$  channels which are highly selective yet capable of high rates of ion transfer.  $Ca^{2+}$  channels use diverse mechanisms of gating, but tend to exhibit similar ion permeability characteristics. According to the earlier mechanism, the factors which define the selectivity of a channel are the energy of hydration of a cation, the energy of coordination by carbonyl oxygen, ionic radius, pore radius, and charge.

## 5.2. Selectivity of Ion Pumps

Ion pumps work in a different way to ion channels. In contrast to ion channels where the high selectivity of binding can slow down the transport of the selected component, i.e.,  $Ca^{2+}$ , ion pumps will transport most efficiently the highly selected ions.  $Ca^{2+}$ ,  $Sr^{2+}$ , and  $Mn^{2+}$  are the only ions that have been demonstrated to be transported by a  $Ca^{2+}$  ATP-ase with the formation of concentration gradients. Sumida et al. [60] studied the effects of other divalent cations on the  $Ca^{2+}$  uptake by microsomes from bovine aortic smooth muscle and indicated

The chain comprises the signature amino acid sequence from bottom to top: T (Threonine), V (Valine), G (Glycine) and Y (Tyrosine), G (Glycine)

Two  $K^+$  ions (green) located at opposite ends of the selectivity filter with a single water molecule in between. The inner ion is depicted in rapid equilibrium between adjacent coordination sites.

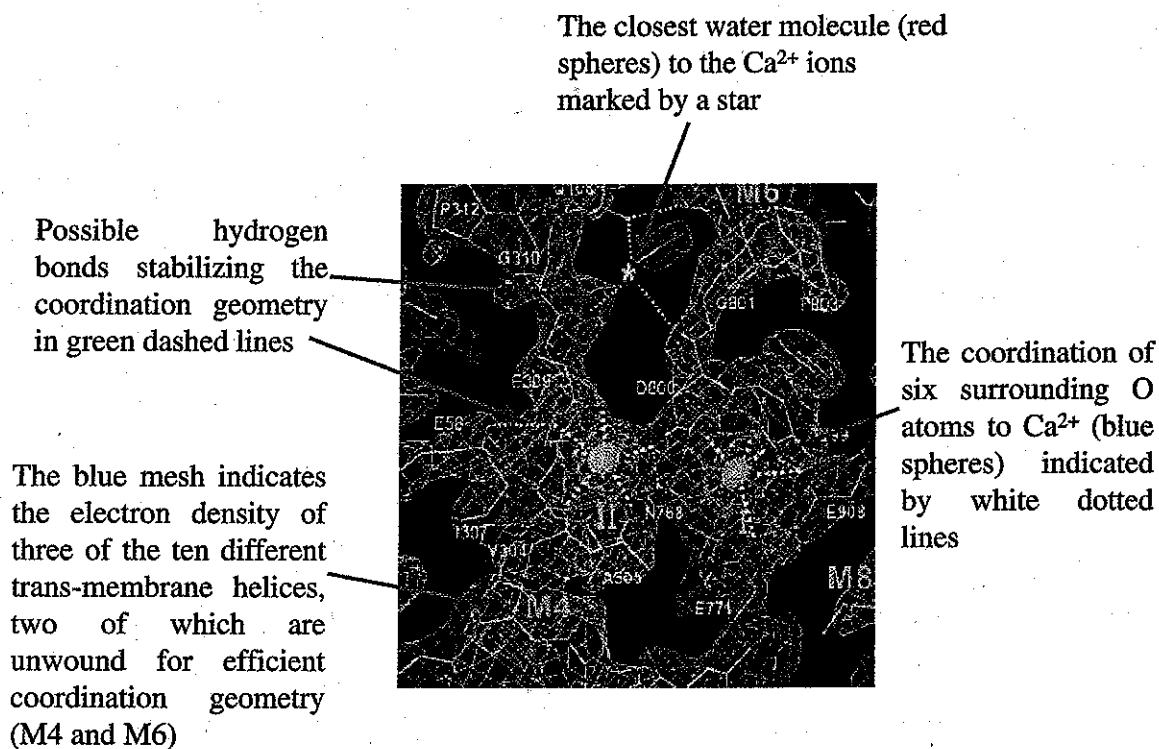
The filter is surrounded by inner and pore helices (white)



The V and Y side chains are directed away from the ion conduction pathway

The ion conduction pathway is lined by the main chain carbonyl oxygen atoms shown here in red

**Figure 6** The selectivity filter of a  $K^+$  channel shown as a stick representation with the chain closest to the viewer removed. The three chains represented are comprised of signature amino acid sequences threonine, valine, glycine, tyrosine, from bottom to top. The selectivity of the pore is controlled by the coordination of side chain carbonyl oxygen from amino acid groups. Adapted from Ref. [59].



that  $\text{Co}^{2+}$ ,  $\text{Zn}^{2+}$ ,  $\text{Mn}^{2+}$ ,  $\text{Fe}^{2+}$ , and  $\text{Ni}^{2+}$  did not interfere with  $\text{Ca}^{2+}$  uptake not the formation of the phosphorylated intermediate and hence, were not in competition with  $\text{Ca}^{2+}$  transport.  $\text{Cd}^{2+}$  however, inhibited both  $\text{Ca}^{2+}$  uptake and the formation of the phosphorylated intermediate but in a non-competitive manner.

The best analogue for  $\text{Ca}^{2+}$  during transport by  $\text{Ca}^{2+}$  ATPase is  $\text{Sr}^{2+}$ , as  $\text{Sr}^{2+}$  can replace  $\text{Ca}^{2+}$  at the binding site. The  $\text{Ca}^{2+}$  ATPase has a higher affinity for  $\text{Ca}^{2+}$  than for  $\text{Sr}^{2+}$  [61]. A simple mechanism for catalysis of transport of two calcium ions which is coupled to the hydrolysis of ATP has been investigated for the relative efficiency of transport of  $\text{Sr}^{2+}$  vs.  $\text{Ca}^{2+}$ . The first step is the binding of two calcium ions to the exterior side of the vesicles. This binding has a high affinity for Ca with  $K_{0.5} \sim 1 \mu\text{M}$ ; the binding of Sr occurs with a lower affinity of  $K_{0.5} \sim 83 \mu\text{M}$  [62]. Overall, the mechanism for the transport of  $\text{Sr}^{2+}$  appears to be the same as that for  $\text{Ca}^{2+}$  and occurs at a similar rate but with a lower affinity by two orders of magnitude.

The best studied  $\text{Ca}^{2+}$  ATPase to date is the skeletal muscle sarcoplasmic reticulum calcium ATPase (SERCA ATPase) which has been characterized to 2.6 Å detail and shows a high degree of specificity for the transported ion (Fig. 7 [63]). The protein consists of 10 helices which conform to allow the  $\text{Ca}^{2+}$  ion to enter, be transported across the membrane and then leave. The specificity seems to arise from the coordination geometry of six oxygen atoms which coordinate the  $\text{Ca}^{2+}$  ion. Interestingly, the six oxygen atoms are located at a distance of 2.2–2.6 Å from the center of each site. This distance can be compared with the Ca–O distance in a calcite crystal of 2.359 Å. This implies that the coordination of the biological cations is controlled in a remarkably similar way to  $\text{Ca}^{2+}$  in a crystal. Furthermore, rows of main chain carbonyl oxygen within helices point towards the cytoplasm and provide a hydrophilic pathway leading to the  $\text{Ca}^{2+}$  binding sites. The rows constrict near the  $\text{Ca}^{2+}$  binding sites, trapping a water molecule. This geometry must be required for displacing water molecules from the  $\text{Ca}^{2+}$ . In a similar way to the mechanism of selectivity for  $\text{Ca}^{2+}$  channels, the selectivity of a  $\text{Ca}^{2+}$  pump is defined by the energy of dehydration and ease to strip water molecules, the energy of binding of the  $\text{Ca}^{2+}$  to the specific site

**Figure 7** An extract of the crystal structure of the calcium ATPase of skeletal muscle sarcoplasmic reticulum at 2.6 Å resolution with two calcium ions bound in the transmembrane domain defined by the electron density map. The two calcium ions are located side by side and are surrounded by four transmembrane helices, two of which are unwound for efficient coordination. The binding site has a highly defined geometry which makes it a high-affinity  $\text{Ca}^{2+}$  binding site due to the coordination of six oxygen atoms from the side chain oxygen atoms of asparagine, glutamate, threonine, aspartic acid, and glycine. This kind of coordination geometry is only possible due to unwinding of the helices. In ATPases that transport heavy metals, the glutamate residue is replaced by cysteine or histidine. The two sites are stabilized by hydrogen-bond networks between the coordinating residues and between residues on other helices. These hydrogen-bond networks must be important for the cooperative binding of two  $\text{Ca}^{2+}$  ions. Adapted from Ref. [63].

denoted by sixfold oxygen coordination from carbonyl oxygen, ionic radius, and charge.

Ca pumps have been demonstrated to be present in most coccolith membranes [64] and identified in the coccolith vesicle membrane [65]. By association these pumps are inferred to be involved in the calcification process. Al-Horani et al. [66] confirmed that corals pump  $\text{Ca}^{2+}$  into the calcifying space using the enzyme  $\text{Ca}^{2+}$  ATPase. No  $\text{Ca}^{2+}$  pump in biomineralization has been characterized for its characteristics of trace metal selectivity. We can only conclude that it is likely that pumps exhibit a strong selectivity between  $\text{Ca}^{2+}$  and all trace metals during biomineralization according to the mechanism outlined earlier.

### 5.3. Selectivity of Acidic Polysaccharide Template

The organic matrix is a preformed insoluble macromolecular framework that is a key mediator of controlled biomineralization. The matrix subdivides the mineralization spaces, acts as a structural framework for mechanical support, and is interfacially active in nucleation [67]. The matrix is a polymeric framework that consists of a complex assemblage of macromolecules, such as proteins and polysaccharides. In its simplest form the matrix consists of a structural framework of predominantly hydrophobic macromolecules with associated cross-links, onto which are anchored hydrophilic macromolecules that present an active nucleating surface. In many cases, the acidic macromolecules are glycoproteins which are proteins with covalently linked polysaccharide side chains that often contain sulfate and carboxylic acid residues [e.g., Fig. 8(C)].

The central role of the organic matrix in controlling inorganic nucleation is to lower the activation energy by reducing the interfacial energy. Lowering of the activation energy for nucleation is considered to arise from the matching of charge polarity, structure, and stereochemistry at the interface between an inorganic nucleus and an organic macromolecular surface. This leads to control over the rate of nucleation, the number and organization of nucleation sites, polymorph selectivity, and oriented nucleation.

The role of any organic template in the calcification of corals remains questionable, and very little is known about the template used by foraminifera. However, the ease of manipulation of coccolithophores in the laboratory has yielded detailed characterization of the acidic polysaccharides which are involved in nucleation and molding of calcite precipitation. Furthermore, the close relationship between the organic matrix and the coccolith has been demonstrated using the new NanoSIMS technique [Fig. 8(A) and (B)]. Future research is planned to use the high resolution chemical abilities of this technique to map out trace metal distributions in the calcite associated with the organic matrix. Three polysaccharides have been identified as being involved in the precipitation of coccolith calcite. Polysaccharide 1 and 2 (PS1 and PS2) form 20 nm particles with  $\text{Ca}^{2+}$  ions and attach to the base plate rim [43]. PS2 probably facilitates calcite nucleation whilst PS3 (in *Pleurochrysis*) or coccolith polysaccharide (in *Emiliania huxleyi*) is a sulfated galacturonan (Fig. 8(C)) [68,69] which is directly linked to

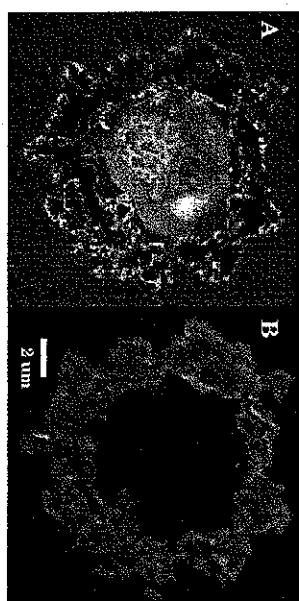
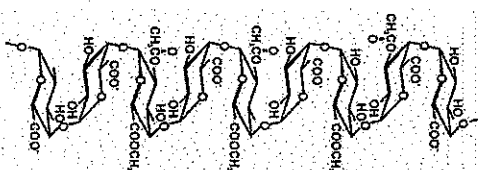


**Figure 8** (A)  $^{12}\text{C}^{14}\text{N}^-$  image of a thin (1  $\mu\text{m}$ ) section of a cryofixed resin embedded *Coccolithus pelagicus* cell obtained with the  $\text{Cs}^+$  ion beam of the Oxford NanoSIMS. The  $\text{CN}^-$  beam depicts the cell and resolves intracellular compartments and the intricate relationship between the organic template and calcite. The calcified cell has a diameter of 12.5  $\mu\text{m}$ . (B) An  $^{16}\text{O}^-$  image of the same cell. The  $^{16}\text{O}^-$  is produced only in the areas where calcite is present and shows the external calcite platelets encircling the cell. (C) The chemical structure of a galactosyluronic acid residue (Gal) which forms part of the acidic polysaccharide involved in calcification separated and identified from coccolithophores.



**C. Gal**

the growth and shaping of coccolith calcite. PS3 from *Pleurochrysis carterae* and *E. huxleyi* share a similar structure of a backbone of mannose residues bearing ester sulfate groups and many galacturonic acid-containing side chains. In a similar manner to the pumps and the channels, the selectivity for nucleation by the template will be controlled by the differential energy of binding of the cations to coordinating oxygen ligands from the acidic polysaccharide.

### 5.4. Biomineralization Selectivity: A Hypothesis

The biological selectivity of the transporters and matrix is strikingly similar in its base chemistry to the selective assembly of ions into a crystal. In each case the selectivity between  $\text{Ca}^{2+}$  and trace metals derives from the balance between the energy required for dehydration of the hexaqua complex of the cation, and the energy released from the new coordination geometry of binding with either carbonyl oxygen from polysaccharides or amino acids, or carbonate oxygen in the crystal. It is remarkable to note that the distance of  $\text{Ca}-\text{O}$  in the site of  $\text{Ca}^{2+}$  ATPase is 2.2–2.6 Å compared with the  $\text{Ca}-\text{O}$  bond length in

**Table 2** Hydration Energy, Electronegativity, and M–O Bond Length for Cations Found Commonly in Biological Calcites

Metal	Gibbs free energy of formation of aqueous ions (kJ/mol) [80]	Electronegativity (Pauling scale)	Bond length M–O in calcite or aragonite structure (Å)
Ca <sup>2+</sup>	–553.6	1.0	2.36
Sr <sup>2+</sup>	–557.3	1.0	2.57–2.73
Ba <sup>2+</sup>	–560.8	0.9	2.74
Mg <sup>2+</sup>	–454.8	1.2	2.11
Mn <sup>2+</sup>	–223.3	1.5	2.19
Zn <sup>2+</sup>	–147.2	1.6	2.11
Cd <sup>2+</sup>	–77.6	1.7	

calcite of 2.359 Å (other M–O bond lengths are quoted in Table 2) which shows how the size of the crystal binding site is mimicked by biology.

However, the size of the binding site in a biological macromolecule or crystal relative to the ionic radius cannot be the only control on trace metal partitioning. From Fig. 1, it is necessary to explain why biological selectivity appears to be more efficient than crystals for cations of a smaller ionic radius and less efficient than crystals for ions larger than Ca<sup>2+</sup>. One possibility arises from the different energies of hydration of the cations (Table 2). The Gibbs free energy of formation of aqueous ions of Ca<sup>2+</sup>, Sr<sup>2+</sup>, and Ba<sup>2+</sup> differ by only 1.3% and Sr<sup>2+</sup> and Ba<sup>2+</sup> are both incorporated preferentially into biological calcite than inorganic calcite. Mg<sup>2+</sup> is the next most similar but releases significantly less energy on hydration (18%). Therefore both sides of the energy balance required for Ca<sup>2+</sup> transport are disrupted by it either in a channel or a pump. Not only will the cations smaller than Ca<sup>2+</sup> bind less favorably at the oxygen-coordinated specific site, but the energy required for dehydration of the cation before specific binding and transport is significantly different to that for Ca<sup>2+</sup>. This idea is speculative at the moment, but could be tested using theoretical chemical calculations for the reaction Gibbs free energies. Furthermore, as calcifying organisms rise to the top of the agenda for genetic DNA sequencing, we anticipate identification of the sequence of the Ca transporting proteins and their closest analogies which will enable direct experimentation on selectivity of transporters from the coccolithophores, foraminifera, and corals.

## 6. BIOLOGICAL ION SELECTIVITY AND THE ENVIRONMENT

All partition coefficients are sensitive to environmental factors including temperature, growth rate or calcification rate and even pH or carbonate ion content of the precipitating media. Whilst we would expect the equilibrium constant of inorganic

carbonate equilibria reactions to be affected by the temperature or pressure of the reaction, the sensitivities of trace metal incorporation to these environmental factors departs extensively from inorganic calcite predictions (Fig. 2).

It is worth mentioning here that the biological sensitivity to the environment or "vital effect" is nothing magical. As outlined earlier the dominant controls on ion selectivity by transporters or the matrix hinges on dehydration of the cation and coordination or bonding by oxygen atoms from neighboring amino acids of a macromolecular protein, which is analogous to the binding site within a calcite or aragonite crystal where a cation is dehydrated and then coordinated by six or nine oxygens of neighboring carbonates, respectively. However, it is important to remember that the utility of the chemistry of biogenic carbonate as proxies for past ocean conditions rests on the observed correlations of the chemistry with environmental variables. If such a correlation does not reflect an inorganic mechanism, it must be due to some biochemical process. Here, we explore how environmental factors might control the biochemical discrimination.

### 6.1. Temperature

Very few studies have investigated the effects of temperature on the selectivity of Ca<sup>2+</sup> ATPases, or Ca<sup>2+</sup> channels as the majority of systems of interest are in warm-blooded mammals which maintain a constant body temperature. Nonetheless, we can create a hypothetical model for the selectivity of channels, pumps, and templates based on the activation energy of binding. It should be noted that Ca<sup>2+</sup> transporters show complex kinetics due to changes in the activation energy of transport, generally characterized by non-linear Arrhenius and van't Hoff plots, but also due to temperature having a great control over the fluidity of the bilayered lipid membrane [70].

If we imagine a Ca<sup>2+</sup> channel which has high selectivity at binding but as a result inhibits large ion currents of the highly specific ion, then the activation energy for the transport of Ca<sup>2+</sup> is higher than the similarly sized trace metals. By contrast, if we imagine a Ca<sup>2+</sup> pump which has high selectivity for both binding and transport, then the activation energy for the transport of Ca<sup>2+</sup> will be lower than that for the similarly sized trace metals. In each case, as temperature increases, the differential between the two activation energies for transport of Ca<sup>2+</sup> and a trace metal becomes less important. Therefore, for biomineralization where Ca<sup>2+</sup> channel processes are dominant we would expect the M/Ca ratio to decrease with increasing temperature, and for biomineralization where Ca<sup>2+</sup> pumps are more important, we would expect the M/Ca ratio to increase as the selectivity breaks down. So, we propose that positive or negative correlation between trace metal uptake and temperature may be due to the differing importance of channels or pumps in the biomineralization process.

Following the previous logic, we would expect the temperature control on the ordering of ions by the organic matrix or template to be similar to that of a Ca<sup>2+</sup> pump. The binding is controlled by lowering the activation energy of

binding for calcium in particular and would be higher for other trace metals. As temperature increases, we expect the  $\text{Ca}^{2+}$ -specific ligands to lose their rigidity and as such reduce the selectivity of the nucleation sites such that the  $\text{M}/\text{Ca}$  ratio will increase with increasing temperature.

## 6.2. Kinetics

Increasingly, growth rate is recognized as controlling the trace metal uptake into biogenic carbonate, and particularly coccolithophores [34–36, 71]. Furthermore, the carbonate ion in the surrounding media controls the degree of calcification and mass of carbonate precipitated for planktonic foraminifera, coccolithophores, and corals [72–74]. A further interlinking proposal is that the trace metal uptake is controlled by the carbonate ion, as demonstrated in benthic foraminifera [75, 76], and proposed for planktonic foraminifera [77]. As the rate of growth or calcification increases in each case, be it driven by carbonate ion or not, the incorporation of the trace metal increases. We propose that this biological rate or kinetic control on trace metal uptake can be considered as a biological analogue of the inorganic model proposed by Lorens [78]. In his model, he proposes a rate-dependent discrimination by the crystal against ions of a different size to  $\text{Ca}^{2+}$ . We propose that trace metal incorporation into biogenic carbonates is

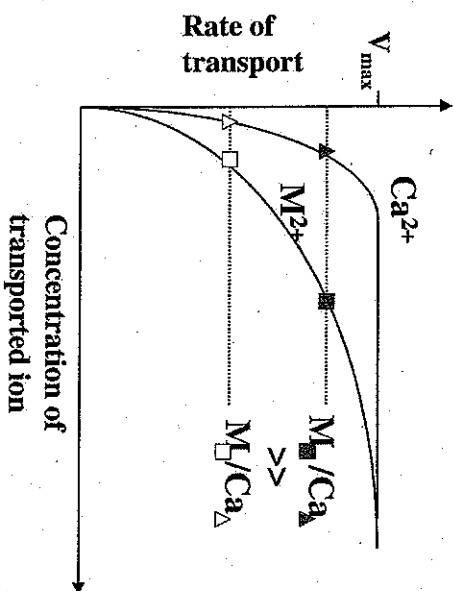


**Figure 9** A hypothetical plot of rate of transport of an ion by a  $\text{Ca}^{2+}$  transporter vs. the concentration of the transported ion for  $\text{Ca}^{2+}$  (triangles) and  $\text{M}^{2+}$  (squares). The slightly higher charge density of the calcium ion relative to the metal ion leads to stronger bonding of the calcium ion by the transporter and more efficient transport at lower concentrations. As the rate of transport of ions increases from the open shapes to the gray shapes, the  $\text{M}/\text{Ca}$  rate of the transported ions will also increase as marked by the dotted lines.

controlled by a rate-dependent discrimination of binding by the transport and template macromolecules.

In channels, pumps or template, there is a binding site specific to the transported ion, namely calcium. In each case,  $\text{Ca}^{2+}$  will be bound more strongly than the trace metal ions [79]. This means that the maximal rate of transport by a  $\text{Ca}^{2+}$  pump or channel ( $V_{max}$ ) would be attained at a lower concentration of  $\text{Ca}^{2+}$  than of the trace metal (Fig. 9). As the rate of transport increases, the concentration of the transported trace metal increases proportionally more than the  $\text{Ca}^{2+}$ . The  $\text{M}/\text{Ca}$  rate transported to the vesicle and available for precipitation will increase with increased rates of pumping. At higher rates, the discrimination between  $\text{Ca}^{2+}$  and trace metals to the nucleation sites of the organic template will be less efficient. In essence, at higher rates of reaction, more mistakes will be made and each process in the biomineralization process is likely to enhance incorporation of trace metals at higher rates of growth or precipitation.

## 7. SUMMARY

Trace-metal proxies bound within the calcium carbonate tests of oceanic organisms provide a unique insight into how the climate system works on timescales which span eight orders of magnitude, from annual to hundreds of millions of years. Whilst the motivation for developing these proxies was the idea that thermodynamic equilibria control the chemistry during precipitation, in reality the application of trace metal proxies relies upon empirical calibration. Such calibration can be applied to a wide range of environmental reconstructions, but more accurate application of proxies requires a mechanistic understanding of the biomineralization process.

The partitioning of trace metals into biogenic carbonates reflects to some extent the same pattern as an inorganic crystal, but there is an additional selectivity and differing environmental sensitivity to, e.g., temperature, which confirms that biochemical processes also play a role in the uptake and assembly of ions into a crystal. Different organisms display differing degrees of biological control on their carbonate chemistry. Aragonitic coral chemistry is most similar to inorganic precipitation from seawater whilst coccolithophores are most different, and these contrasts correlate with the degree of control of the organism over its biomineralization.

Selectivity between Ca and trace metals during biomineralization arises during transport by pumps, channels, or nucleation upon an organic matrix. The biological selectivity of the transporters and matrix is strikingly similar in its base chemistry to the selective assembly of ions into a crystal. In each case, the selectivity between  $\text{Ca}^{2+}$  and trace metals derives from the balance between the energy required for dehydration of the hexaqua complex of the cation, and the energy released from the new coordination geometry of binding with either carbonyl oxygen from polysaccharides or amino acids, or carbonate oxygen in the crystal. This is a speculative idea, but with some careful chemical



calculations based on the energy of binding of  $\text{Ca}^{2+}$  or the trace metal ions to these macromolecular structures, it provides an alternative thermodynamic framework within which to consider the application of trace metal proxies.

## ACKNOWLEDGMENTS

R. Rickaby acknowledges the support of the Natural Environmental Research Council grant number: NER/M/S/2002/00123 and is also grateful for constructive discussions with Sam Shaw, Nick Belshaw, and Don Fraser.

## ABBREVIATIONS

AABW	Antarctic bottom water
$\delta^{20}\text{O}$	isotopic variation of the element $^{20}\text{O}$ , e.g., of $^{18}\text{O}$ , relative to an internationally accepted standards in parts per thousand or per mill
kyr	kilo years
MC-ICPMS	multi-collector inductively coupled plasma mass-spectrometry
Myr	million years
NADW	North Atlantic deep water
PS	polysaccharide
SEM	scanning electron microscopy
SERCA	skeletal muscle sarcoplasmic reticulum calcium ATPase
SI	International System of Units
SIMS	secondary ion mass spectrometry

## REFERENCES

1. Urey HC. *J Chem Soc* 1947; 562-581.
2. Epstein S, Buchsbaum HA, Lowenstam HA, Urey HC. *Bull Geol Soc Am* 1953; 64:1315-1326.
3. Bemis BE, Spero HJ, Bijma J, Lea DW. *Paleoceanography* 1998; 13:150-160.
4. Boyle EA. *Earth Planet Sci Lett* 1981; 53:11-35.
5. Croal LR, Johnson CM, Beard BL, Newman DK. *Geochim Cosmochim Acta* 2004; 68:1227-1242.
6. Icopini GA, Anbar AD, Rieubush SS, Tien M, Brantley SL. *Geology* 2004; 32:205-208.
7. Arnold GL, Anbar AD, Barling J, Lyons TW. *Science* 2004; 304:87-90.
8. Siebert C, Nagler TF, von Blanckenburg F, Kramers JD. *Earth Planet Sci Lett* 2003; 211:159-171.
9. Anbar AD. *Earth Planet Sci Lett* 2004; 217:223-236.
10. Elderfield H, Rickaby REM. *Nature* 2000; 405:305-310.
11. Boyle EA, Keigwin LD. *Earth Planet Sci Lett* 1985/86; 76:135-150.
12. Anand P, Elderfield H, Conte MH. *Paleoceanography* 2003; 18:art. no. 1050.
13. Rosenthal Y, Oppo DW, Linsley BK. *Geophys Res Lett* 2003; 30:art. no. 1428.
14. Schmidt MW, Spero HI, Lea DW. *Nature* 2004; 428:160-163.
15. Palmer MR, Elderfield H. *Nature* 1985; 314:526-528.
16. Holland HD. *Prog. Rep. U.S. AEC Contract No. AT (30-1), 2266 (1960)*.
17. Holland HD, Borsik M, Munoz J, Oxburgh UM. *Geochim Cosmochim Acta* 1963; 27:957-977.
18. Kinsman DJ, Holland HD. *Geochim Cosmochim Acta* 1969; 33:1-17.
19. Driessens FCM. *ACS Symp Ser* 1986; 323:524-560.
20. Svefjensky DA. *Geochim Cosmochim Acta* 1984; 48:1127-1134.
21. Svefjensky DA. *Geochim Cosmochim Acta* 1985; 49:853-864.
22. Rimsditch JD, Balog A, Webb J. *Geochim Cosmochim Acta* 1998; 62:1851-1863.
23. Lea DW. *Trace Elements in Foraminiferal Calcite*. In: Sen Gupta B, ed. *Modern Foraminifera*. Dordrecht: Kluwer, 1999:259-277.
24. Shen GT, Dunbar RB. *Geochim Cosmochim Acta* 1995; 59:2009-2024.
25. Lea DW. *Elemental and Isotopic Proxies of Marine Temperatures*. In: Elderfield H, ed. *The Oceans and Marine Geochemistry*. Vol. 6. *Treatise on Geochemistry*. Holland HD and Thierckan KK, eds. Oxford: Elsevier-Pergamon, 2003; 365-390.
26. Weiner S, Dove PM. *Rev Mineral Geochem* 2003; 54:1-29.
27. Henderson GM. *Earth Planet Sci Lett* 2002; 203:1-13.
28. Linn LJ, Delaney ML, Druffel BRM. *Geochim Cosmochim Acta* 1990; 54:387-394.
29. Delaney ML, Linn LJ, Druffel BRM. *Geochim Cosmochim Acta* 1993; 57:347-354.
30. Renner MK, Boyle EA, Cole JE. *Earth Planet Sci Lett* 2003; 210:437-452.
31. Linsley BK, Wellington GM, Schrag DP, Ren L, Salinger MJ, Tudhope AW. *Clim Dyn* 2004; 22:1-11.
32. Skinner LC, Shackleton NJ, Elderfield H. *Geochim Geophys Geosys* 2003; 4:art. no. 1098.
33. Keigwin LD, Boyle EA. *Paleoceanography* 1999; 14:164-170.
34. Stoll HM, Kias CM, Probert I. *Glob Planet Change* 2002; 34:153-171.
35. Stoll HM, Rosenthal Y, Falkowski P. *Geochim Cosmochim Acta* 2002; 66:927-936.
36. Rickaby REM, Schrag DP, Zondervan I, Riebesell U. *Glob Biogeochem Cycles* 2002; 16:art. no. 1006.
37. Stoll HM, Bains S. *Paleoceanography* 2003; 18:art. no. 1049.
38. Bailey TR, Rosenthal Y, McArthur JM, van de Schootbrugge B, Thirwall MF. *Earth Planet Sci Lett* 2003; 212:307-320.
39. Westbroek P, Vandervel P, Borman AH, Devriend JPM, Kok D, Debruijn WC, Parker SB. *Phil Trans R Soc Lond B* 1984; 304:435-444.
40. Slinkins K, Wilbur KM. *Biomimetalization: Cell Biology and Mineral Deposition*. San Diego, CA: Academic Press, 1989.
41. Lowenstam HA, Weiner S. *On Biomimetalization*. New York: Oxford University Press, 1989.
42. Young JR, Henriksen K. *Rev Mineral Geochem* 2003; 54:189-215.
43. Marsh ME. *Protoplasma* 1994; 177:108-122.
44. Young JR, Didymus JM, Bown PR, Pitus B, Mann S. *Nature* 1992; 356:516-518.
45. Erez J. *Rev Mineral Geochem* 2003; 54:115-149.
46. Anderson OR, Faber WW. *J Forum Res* 1984; 14:303-308.
47. Erez J, Benov S, Brownlee C, Raz M, Rinkevich B. *Geochim Cosmochim Acta* 2002; 66(suppl 1): A216-A216.

48. Cohen AL, McConaughy TA. *Rev Mineral Geochem* 2003; 54:151-187.
49. Hayes RL, Goreau NJ. *Biol Bull* 1977; 152:26-40.
50. Constanz BR. Skeletal organisation in Acropora. In: Crick RE, ed. *Origin, Evolution and Modern Aspects of Biomineralization in Plants and Animals*. New York: Plenum Press, 1989:175-200.
51. Ip YK, Krishnaveni P. *J Exp Zool* 1991; 258:273-276.
52. Ferrier-Pages C, Boisson F, Allemand D, Tambutte E. *Mar Ecol-Progr Ser* 2002; 245:93-100.
53. Barnes DI. *Science* 1970; 170:1305-1308.
54. Constanz BR. *Palaios* 1986; 1:52-157.
55. Cui JP, Lecointre G, Perrin C, Tiller A, Tiller S. *Zoologica Scripta* 2003; 32:459-473.
56. Hagiwara S, Byerly L. *Ann Rev Neurosci* 1981; 4:69-125.
57. Almers W, Palade PT. *J Physiol-Lond* 1981; 312:159-176.
58. Hess P, Lansman JB, Tsien RW. *J Gen Physiol* 1986; 88:293-319.
59. Doyle DA, Cabral JM, Pfuetschner RA, Kuo AL, Gulbis JM, Cohen SL, Chait BT, MacKinnon R. *Science* 1998; 280:69-77.
60. Sumida M, Hamada M, Takenaka H, Hirata Y, Nishigauchi K, Okuda H. *J Biochem* 1986; 100:765-772.
61. Yu X, Inesi G. *J Biol Chem* 1995; 270:4361-4367.
62. Fujimori T, Jencks WP. *J Biol Chem* 1992; 267:18466-18474.
63. Toyoshima C, Nakasako M, Nomura H, Ogawa H. *Nature* 2000; 405:647-655.
64. Kwon DK, Gonzalez EL. *J Physiol* 1994; 30:689-695.
65. Araki Y, Gonzalez EL. *J Physiol* 1998; 34:79-88.
66. Al-Horani FA, Al-Moghrabi SM, de Beer D. *Mar Biol* 2003; 142:419-426.
67. Mann S. *Biomineralization: Principles and Concepts in Bioinorganic Materials Chemistry*. New York: Oxford University Press, 2001.
68. Fichtinger-Schepman AMJ, Kamerling JP, Versluis C, Vliegenthart JFG. *Carbohydr Res* 1981; 93:105-123.
69. Marsh ME, Ridall AL, Azadi P, Duke P. *J Struct Biol* 2002; 139:39-45.
70. Caldwell CR, Hang A. *Physiol Plant* 1981; 53:117-124.
71. Stoll HM, Schrag DP. *Geochim Geophys Geosys* 2000; 1:1999GC000015.
72. Kleygas JA, Buddemeier RW, Archer D, Gattuso JP, Langdon C, Opdyke BN. *Science* 1999; 284:118-120.
73. Barker S, Elderfield H. *Science* 2002; 297:833-836.
74. Riebesell U, Zondervan I, Rost B, Tortell PD, Zeebe RE, Morel FMM. *Nature* 2000; 407:364-367.
75. McCorkle DC, Martin PA, Lea DW, Klinkhammer GP. *Paleoceanography* 1995; 10:699-714.
76. Marchitto TM, Curry WB, Oppo DW. *Paleoceanography* 2000; 15:299-306.
77. Boyle EA, Erez J. *EOS Trans. AGU* 84 (52) Ocean Sci Meet Suppl 2004; Abstract OS21G-01.
78. Lorenz RB. *Geochim Cosmochim Acta* 1981; 45:553-561.
79. Stephan S, Hasselbach W. *Eur J Biochem* 1991; 196:231-237.
80. Stark JG, Wallace HG. *Chemistry Data Book*, in *International System of Units (SI)*. 2d ed. London: John Murray Ltd, 1990.

## Subject Index

- A.
  - eutrophus*, see *Alcaligenes haemolyticus*, see *Acinetobacter hallii*, see *Arbidiopsis putrefaciens*, see *Alteromonas thalassia*, see *Arbidiopsis*
  - AAS, see Atomic absorption spectroscopy
  - F-, see Flame atomic absorption spectroscopy
  - GF-, see Graphite furnace atomic absorption spectroscopy
  - Acetate
    - as ligand, 50
  - Achillea ageratum*, 189
  - Acid volatile sulfide model, 67, 68
  - Acinetobacter haemolyticus*, 34
  - Acinetoferrin, 34
  - structure, 36
  - Actinides (see also individual elements), 209-211, 215, 219-227
  - bioremediation, see Bioremediation interaction with microorganisms, 220-227
  - oxidation states, 212, 221
  - redox potential, see Redox potentials
  - Adenosine 5'-triphosphate, see 5'-ATP
- Aerobactin, 29
- ferric, 26
- structure, 30
- Aerosols (containing) (see also Air and Atmosphere)
  - analysis, 15
  - antimony, 185
  - from industry, 10
  - lead, 3
  - marine, 6
  - Mediterranean, 185
  - metals, 4, 10, 12
  - North Atlantic, 185
  - Saharan dust, 185
  - soil-derived, 11
- Affinity constants, see Stability constants
- Africa
  - antimony in atmosphere, 184
  - gold production, 10
  - mercury emission, 10
- AFS, see Atomic fluorescence spectrometry
- Agriculture
  - pesticide, see Pesticides
- Air (see also Atmosphere)
  - antimony in, 183, 185
  - pollution, 15
  - sources of metals, 6-13
- Alaska
  - arsenic in soil, 147
  - Baffin Island, 147